

Three-body systems with attractive $1/r$ potentials

J. P. D’Incao, S. C. Cheng, H. Suno and B. D. Esry

Department of Physics, Kansas State University, Manhattan, Kansas 66506, USA

We have used the hyperspherical adiabatic representation to describe the system of three identical bosons in an spin stretched state interacting by an attractive $1/r$ potential. A proposal has been made how such a system might be realized experimentally in cold trapped atoms using extremely off-resonant laser fields [Phys. Rev. Lett. 84, 5687 (2000)]. We have obtained effective potentials, channel functions, and nonadiabatic couplings for this gravity-like interaction, allowing us to calculate the ground state energy with accuracy that substantially improves upon previous results. We have similarly calculated the energies for the first four 0^+ excited states. These results show that the simple adiabatic hyperspherical approximation offers an accurate description for such a system.

PACS numbers: 31.15.Ja, 32.10.-f, 34.20.Cf

I. INTRODUCTION

Recently, a scheme for inducing gravitation-like interatomic potentials has been proposed [1], opening up the possibility to create self-bound Bose-Einstein condensates (BECs) [2, 3, 4, 5, 6]. In such a scheme, the gravitation-like interatomic potential can be achieved by irradiating the atoms with intense, extremely off-resonant electromagnetic fields. The usual strong anisotropy due to dipole-dipole interactions can, in fact, be averaged out [7] by the proper combination of laser beams, leaving a $-u/r$ potential, where u is the strength of the potential (the analogue of GMm , where G is the Newton’s constant and M and m are the masses) and r is the interparticle distance. The strength u of the potential can be adjusted by changing the laser intensity [1].

In ultracold atomic gases, two interesting regimes for self-bound BECs have been predicted, assuming that the short-range interatomic interactions can be independently tuned by, say, applying a magnetic field near a Feshbach resonance [8]. In one regime, the attractive $1/r$ interactions are balanced by the repulsive mean field interaction assuming a positive two-body scattering length and negligible kinetic energy. In the other regime, the balancing factor is kinetic energy, assuming negligible mean field interactions. In both regimes, the resulting BEC is self-bound. From a broader point of view, the induced gravitation-like interaction might make possible experimental emulation of boson stars (a system of self-gravitating bosons) in the regime where the kinetic energy balances the $-u/r$ potential [9, 10]. Moreover, purely attractive $1/r$ potentials constitute an interesting contrast to the attractive *and* repulsive Coulomb potentials atomic physics are used to.

The existence of a lower bound for the ground state energy in many-body systems interacting through attractive $1/r$ potentials is of fundamental importance in order to prove the existence of the thermodynamical limit and the stability of normal matter [11]. It was shown in Ref. [12] that for a system of N identical, spinless (or spin stretched) bosons of mass m interacting gravitation-

ally, the lower and upper bounds for the ground state energy are, respectively, $-\frac{1}{16}N^2(N-1)G^2m^5/\hbar^2$ and $-0.0542N(N-1)^2G^2m^5/\hbar^2$, where the upper bound was obtained variationally. For small N , however, the discrepancy between the lower and upper bounds becomes large. For $N = 3$, using a more refined trial function, they obtained $-0.95492G^2m^5/\hbar^2$ for the upper bound, representing a difference of about 15% between the upper and lower $(-\frac{9}{8}G^2m^5/\hbar^2)$, bounds and a ground state energy equal to $E_0 \cong -1.067G^2m^5/\hbar^2$.

In this paper, we have used the adiabatic hyperspherical representation for this system to obtain effective three-body potentials, the corresponding channel functions, and the nonadiabatic couplings. Using these, we calculate the ground state and low-lying 0^+ excited state energies converged to seven digits. We have also used the adiabatic hyperspherical representation to obtain lower and upper bounds that differ by about 0.1%, indicating that a simple single-channel description offers a quite accurate description of such systems.

II. THE ADIABATIC HYPERSPHERICAL REPRESENTATION

We have solved the Schrödinger equation in hyperspherical coordinates. After separation of the center-of-mass motion, the system is described by the hyperradius R which gives the overall size; three Euler angles α , β and γ , specifying the orientation of the plane containing the three particles relative to the space-fixed frame; and other two hyperangles φ and θ , describing the internal relative motion between the particles. We have defined φ and θ as a modification of Smith-Whitten coordinates [13, 14, 15]. The key to the adiabatic hyperspherical representation is that the dynamics of the three-body system is reduced to collective motion under the influence of one-dimensional effective potentials in R , which is governed by a system of ordinary differential equations.

The hyperspherical coordinates are introduced through the mass-scaled Jacobi coordinates $\vec{\rho}_1$ and $\vec{\rho}_2$ (see Fig. 1)

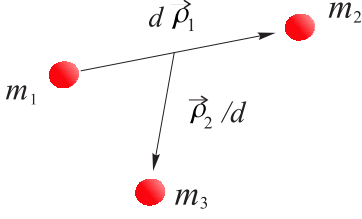


FIG. 1: The mass-scaled Jacobi coordinates for systems with three particles.

defined as

$$\begin{aligned}\vec{\rho}_1 &= (\vec{r}_2 - \vec{r}_1)/d, \\ \vec{\rho}_2 &= d \left(\vec{r}_3 - \frac{m_1 \vec{r}_1 + m_2 \vec{r}_2}{m_1 + m_2} \right).\end{aligned}\quad (1)$$

In the above equations \vec{r}_i is the position of the particle i (of mass m_i) relative to a space-fixed frame. For three identical particles of mass m , we define a three-body reduced mass as $\mu = m/\sqrt{3}$ which gives $d = 2^{1/2}/3^{1/4}$ [14, 15]. It is important to note that the hyperradius,

$$R^2 = \rho_1^2 + \rho_2^2, \quad R \in [0, \infty), \quad (2)$$

is an invariant quantity, i.e., it does not depend on the particular choice of the hyperangles or labels of the particles.

The Schrödinger equation can be more conveniently written in terms of the rescaled wave function $\psi = R^{5/2}\Psi$, as

$$\left[-\frac{\hbar^2}{2\mu} \frac{\partial^2}{\partial R^2} + H_{\text{ad}}(R, \Omega) \right] \psi(R, \Omega) = E\psi(R, \Omega), \quad (3)$$

where E is the total energy and H_{ad} is the adiabatic Hamiltonian given by

$$H_{\text{ad}}(R, \Omega) = \frac{\hbar^2}{2\mu R^2} \left[\Lambda^2(\Omega) + \frac{15}{4} \right] + V(R, \varphi, \theta). \quad (4)$$

The adiabatic Hamiltonian H_{ad} contains all hyperangular dependence, represented collectively by $\Omega \equiv \{\varphi, \theta, \alpha, \beta, \gamma\}$, and includes the hyperangular kinetic energy in the grand angular momentum operator Λ^2 as well as all interparticle interactions V .

In the adiabatic hyperspherical representation, the total wave function is expanded in terms of the channel functions $\Phi_\nu(R; \Omega)$,

$$\psi_n(R, \Omega) = \sum_\nu F_{n\nu}(R) \Phi_\nu(R; \Omega), \quad (5)$$

where $F_{n\nu}(R)$ are the hyperradial wavefunctions, n labels the different energy eigenstates for a given ν , and ν represents all remaining quantum numbers necessary to specify each channel. The channel functions $\Phi_\nu(R; \Omega)$ form a complete set of orthonormal functions at each value of R and are eigenfunctions of the adiabatic Hamiltonian:

$$H_{\text{ad}}(R, \Omega) \Phi_\nu(R; \Omega) = U_\nu(R) \Phi_\nu(R; \Omega). \quad (6)$$

The eigenvalues $U_\nu(R)$ help define effective three-body potentials for the hyperradial motion.

Substituting Eq. (5) into the Schrödinger equation (3) and projecting out $\Phi_{\nu'}$, we obtain the hyperradial Schrödinger equation

$$\left[-\frac{\hbar^2}{2\mu} \frac{d^2}{dR^2} + U_\nu(R) \right] F_\nu(R) - \frac{\hbar^2}{2\mu} \sum_{\nu'} \left[2P_{\nu\nu'}(R) \frac{d}{dR} + Q_{\nu\nu'}(R) \right] F_{\nu'}(R) = EF_\nu(R), \quad (7)$$

which describes the motion of the three-body system under the influence of the effective potentials $U_\nu(R) - Q_{\nu\nu'}(R)/2\mu$. The nonadiabatic coupling terms $P_{\nu\nu'}(R)$ and $Q_{\nu\nu'}(R)$ drive inelastic collisions three-body scattering processes and are defined as

$$P_{\nu\nu'}(R) = \left\langle \Phi_\nu \left| \frac{d}{dR} \right| \Phi_{\nu'} \right\rangle \quad (8)$$

and

$$Q_{\nu\nu'}(R) = \left\langle \Phi_\nu \left| \frac{d^2}{dR^2} \right| \Phi_{\nu'} \right\rangle, \quad (9)$$

where the double brackets denote integration over the angular coordinates Ω only. As it stands, Eq. (7) is exact.

In practice, of course, the sum over channels must be truncated. In fact, the accuracy of the solutions can be monitored with successively larger truncations since the bound state energies obtained at each stage are an upper bound by the variational principle.

In this paper, we explore the solutions of the system of differential equations (7) for three particles with attractive $1/r$ interactions. We determine the effective potentials and couplings by solving Eq. (6) for the $J^\pi = 0^+$ symmetry, where J is the total orbital angular momentum and π is the total parity. The low-lying bound state energies are then determined by solving Eq. (7).

In order to solve the adiabatic equation (6), we have expanded the channel functions $\Phi_\nu(R; \Omega)$ in terms of the

Wigner D functions [14, 16, 17],

$$\Phi_\nu^{JM\pi}(R; \Omega) = \sum_K \phi_{K\nu}(R; \theta, \varphi) D_{KM}^J(\alpha, \beta, \gamma), \quad (10)$$

where K and M are the projection of \vec{J} onto the body-fixed and space-fixed z -axes, respectively. After projecting out the D functions, the resulting coupled system of partial differential equations for $\phi_{K\nu}(R; \theta, \varphi)$ is solved (for each value of R) by expanding $\phi_{K\nu}(R; \theta, \varphi)$ on a direct product of fifth order basis splines [18] in the hyperangles θ and φ [14, 15]. For $J^\pi = 0^+$, of course, the sum involves only one term, requiring the solution of a single two-dimensional partial differential equation.

The potential V in Eq. (4) is given by a pairwise sum of attractive $1/r$ potentials,

$$V(R, \theta, \varphi) = -\frac{u}{r_{12}} - \frac{u}{r_{23}} - \frac{u}{r_{31}}, \quad (11)$$

where u is the gravitation-like coupling. The interparticle distances r_{ij} are given in terms of the hyperspherical coordinates by

$$\begin{aligned} r_{12} &= 3^{-1/4} R [1 + \sin \theta \sin(\varphi - \pi/6)]^{1/2}, \\ r_{23} &= 3^{-1/4} R [1 + \sin \theta \sin(\varphi - 5\pi/6)]^{1/2}, \\ r_{31} &= 3^{-1/4} R [1 + \sin \theta \sin(\varphi + \pi/2)]^{1/2}. \end{aligned} \quad (12)$$

Figure 2 shows the potential $V(R, \theta, \varphi)$ as a function of θ and φ at $R = 100$. The singular points at $\theta = \pi/2$ and $\varphi = \pi/3, \pi$ and $5\pi/3$ are the points where $r_{23} = 0$, $r_{31} = 0$ and $r_{12} = 0$, respectively. Notice that our choice for the hyperangles θ and φ [14, 15] — like any of the so-called democratic or Smith-Whitten coordinates — implies a periodicity of the potential in φ for identical particles, which substantially simplifies the numerical solution of Eq. (6) when symmetrizing the wave function. The two-dimensional equation for $J^\pi = 0^+$ thus needs to be solved only from $\varphi = 0$ to $2\pi/3$, with the requirement that the derivative of $\phi(R; \theta, \varphi)$ with respect to φ is zero at each boundary, followed by postsymmetrization to extract the completely symmetric solutions. We have treated the cusp due the $1/r$ divergence as $r \rightarrow 0$ by including more spline functions [18] at $\varphi = \pi/3$. For other J^π the solutions can be determined in a similar way [14, 15].

In the atomic case, suggested in Ref. [1], u is given by (in S.I. units)

$$u = \frac{11}{4\pi} \frac{I q^2 \alpha_p^2}{c \varepsilon_0^2} \quad (13)$$

where I is the laser intensity, q the photon wave number, and α_p the atomic dynamic polarizability. So, under the conditions discussed in Ref. [1], the strength of the interaction is controllable via the laser's parameters. For the present calculations, however, we base our units on u , thus producing a unitless equation. Our length units are $2\hbar^2/mu$, and our energy units are $mu^2/2\hbar^2$. These yield, in analogy to atomic units, a two-body energy spectrum $E_n = -1/2n^2$.

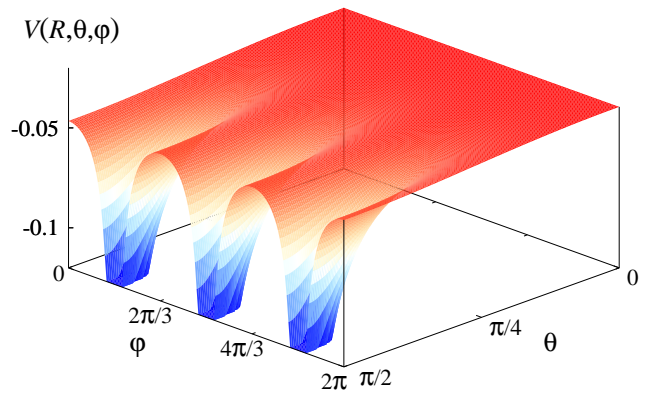


FIG. 2: The potential $V(R, \theta, \varphi)$ at $R = 100$. Due to the symmetry properties of the three identical particles, the adiabatic equation [Eq. (6)] is solved only for $\theta = 0$ to $\pi/2$ and $\varphi = 0$ to $2\pi/3$

III. RESULTS AND DISCUSSION

Figure 3 shows the effective three-body potentials in the form $[-2U_\nu(R)]^{-1/2}$ such that for large values of R they converge to the principal quantum number n_{2b} associated with the two-body hydrogen-like subsystems (for $R \rightarrow \infty$ one particle is far from the others). The lowest potential in Fig. 3, converging to $n_{2b} = 1$, supports the 0^+ bound states (or S^e , in analogy with atomic spectroscopic notation). In particular, it contains both the ground state and the S^e series of singly excited states, using the language of atomic structure. The higher potentials (converging to $n_{2b} > 1$) support series of doubly excited states that are coupled to and can decay to the continuum of the lowest potential and are thus metastable. These comments draw on the similarity of these potentials to those for three-body systems like He and H^- [19]. There are minor differences, of course, due to the different permutational symmetries of the two systems and to the absence of the Coulomb repulsion for the present case.

Since the $J^\pi = 0^+$ channel functions depend only on the hyperangles θ and φ they can be plotted in their entirety for each value of R . Figures 4 and 5 show the channel functions for the two lowest channels at $R = 0.69$ and 100 for $\nu = 1$, and $R = 5.75$ and 100 for $\nu = 2$. The first R value lies near the respective potential minima; and the second, in the asymptotic region. For small R , we plot Φ_ν in the range $0 \leq \varphi \leq 2\pi/3$ from which the function in the whole range $0 \leq \varphi \leq 2\pi$ can be obtained by symmetry (translation of the plotted portion by $2\pi/3$ and $4\pi/3$). For large R , however, we plotted the solution only in the range $\pi/6 \leq \varphi \leq \pi/2$ to emphasize the two-body character of the solution.

The hyperangular distributions are useful because they reveal the geometry of the system. At $\theta = 0$, for instance, the atoms form an equilateral triangle, while for $\theta = \pi/2$

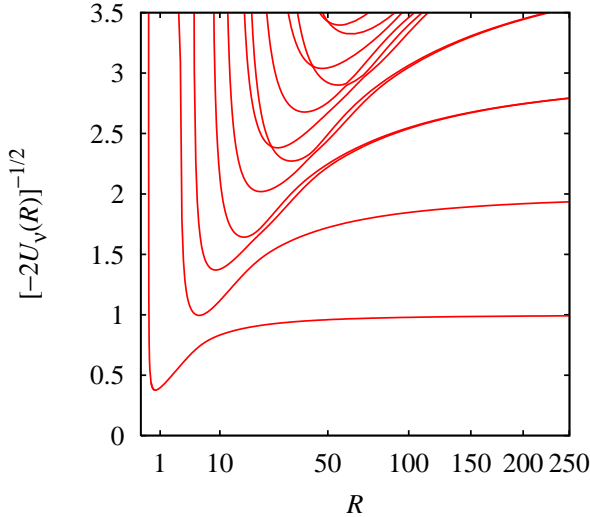


FIG. 3: The hyperspherical potentials for three identical bosons with attractive $1/r$ interactions. For large values of R , $[-2U_\nu(R)]^{-1/2}$ converges to the principal quantum number n_{2b} for the hydrogen-like subsystems.

they lie along a line. Figure 4(a) shows that near the $\nu = 1$ potential minimum (see Fig. 3) the lowest channel function is spread out over the entire hyperangular plane with an increased amplitude near the two-body coalescence point ($r_{31} = 0$) at $\theta = \pi/2$ and $\varphi = \pi/3$. This point corresponds to a linear configuration with two of the particles closer to each other than to the third particle, representing strong two-body correlations. Since this R is the equilibrium distance, the three particles in the ground state thus assume all triangular shapes between linear and equilateral with a preference for linear shapes having two particles close to each other (taking into account the $\sin 2\theta$ volume element). As R increases [Fig. 4(b)] the channel function “collapses” to the region around the coalescence points, displaying the two-body character it must have for $R \rightarrow \infty$ — in this case the $1s$ state. Figures 5(a) and 5(b) show the $\nu = 2$ channel function. They show much the same behavior as $\nu = 1$ except with the necessary addition of a node. Figure 5(b) shows that $\nu = 2$ converges to the $2s$ state of the two-body subsystem. Note that for identical spinless (or spin-stretched) bosons, $2p$ two-body states are not allowed by symmetry, so there is only a single potential correlating to $n_{2b} = 2$ at $R \rightarrow \infty$.

In Figure 6 we show the nonadiabatic couplings $P_{\nu\nu'}(R)$ between the lowest channel and the next three channels ($P_{\nu\nu} = 0$ and $P_{\nu\nu'} = -P_{\nu'\nu}$) calculated from Eq. (9). The fact that the coupling P_{12} in Fig. 6 is substantially larger than the couplings with higher channels implies rapid convergence for the bound state energies as a function of the number of channels. Further, P_{12} peaks around $R = 6$ which correlates roughly with the location of an avoided crossing between the corresponding potential curves as expected (see Fig. 3).

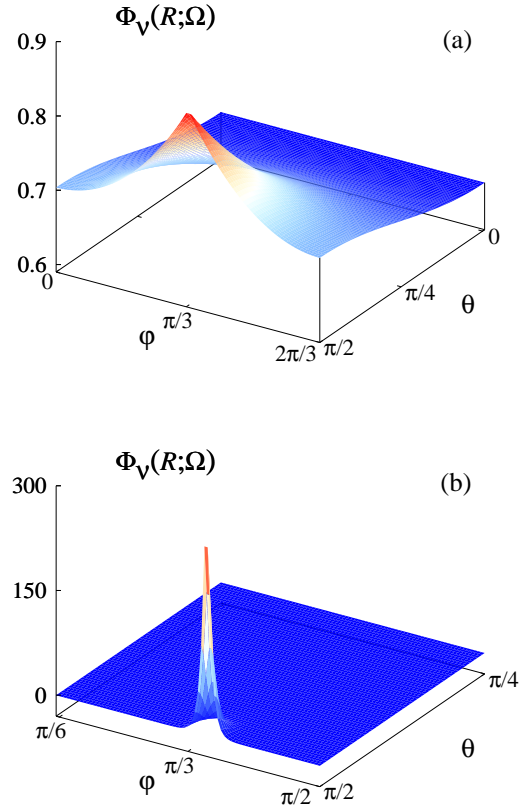


FIG. 4: The lowest $J^\pi = 0^+$ channel function ($\nu = 1$) as a function of θ and φ at (a) $R = 0.69$ and (b) $R = 100$.

We have solved Eq. (7) and determined the bound state energies and hyperradial wavefunctions $F_{n\nu}(R)$ including up to 15 channels. For example, Figure 7 shows the ground state wave function for a three channel calculation. The $\nu = 1$ component is associated with the lowest adiabatic channel, while the $\nu = 2$ and $\nu = 3$ are related to the next two adiabatic channels and are present due to the coupling between the channels. Note that the probability given by $\mathcal{P}_{n\nu} = \int_0^\infty |F_{n\nu}(R)|^2 dR$ due to the first term dominates the other contributions. In Table I we show $\mathcal{P}_{n\nu=1}$ for the ground state ($n = 1$) and the four lowest excited states for a 15 channel calculation. The $\nu = 1$ adiabatic channel represents roughly 99% or more of the probability for each state, showing that the adiabatic expansion is, in fact, quite good.

In Table II we show the ground state energy as a function of the number of channels, further demonstrating the expected rapid convergence of the adiabatic expansion. The ground state energy for this system has certainly been calculated before. In Ref. [12], for instance, a ground state energy of $E_0 \cong -1.067 G^2 m^5 / \hbar^2 = -2.134 mu^2 / \hbar^2$ (in our units) was obtained. Comparison with Table II shows that since both calculations are variational, our single channel calculation already gives a more precise

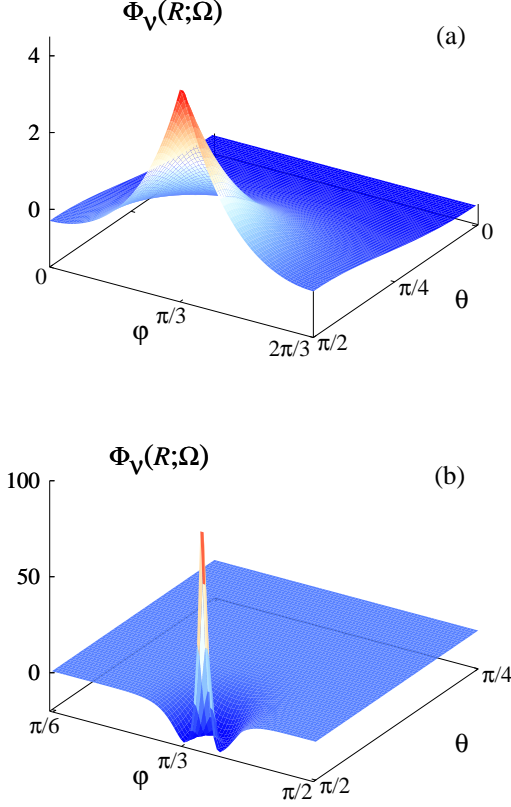


FIG. 5: The first excited $J^\pi = 0^+$ channel function ($\nu = 2$) as a function of θ and φ at (a) $R = 5.75$ and (b) $R = 100$.

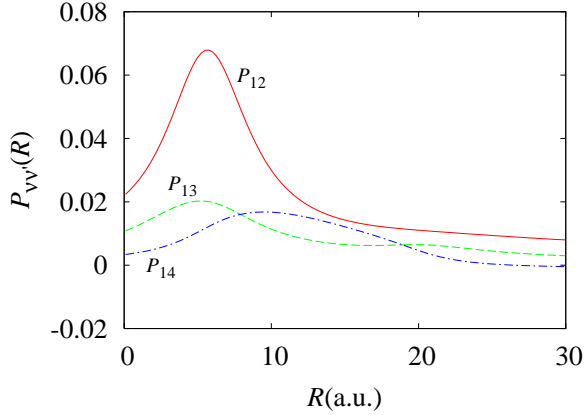


FIG. 6: Nonadiabatic coupling $P_{\nu\nu'}$ between the lowest channel and the next three channels.

result. We speculate that the large differences in the potential energies shown in Fig. 3 are the main reason that a single channel already gives such a good result. In fact, this channel separation is closely related to the small magnitude of the coupling terms shown in Fig. 6. Table II also shows that our six channel approximation for the ground state gives a result converged to seven

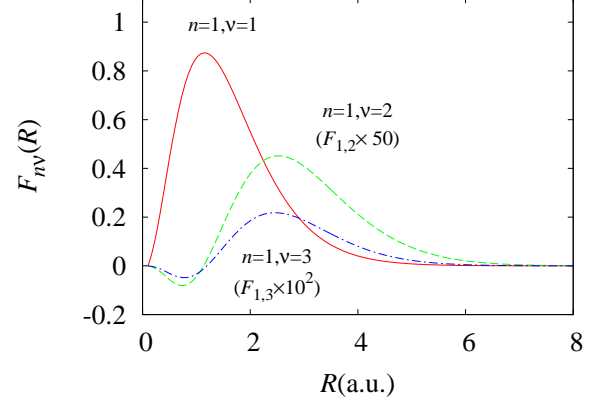


FIG. 7: First three components of the ground state hyperradial wavefunction $F_{n\nu}$ ($n = 1$) associated with the first three channels $\nu = 1, 2$, and 3 .

TABLE I: The probability $\mathcal{P}_{n\nu}$ associated with the $\nu = 1$ term of the expansion (5) for the ground state ($n = 1$) and the next four excited states.

n	$\mathcal{P}_{n1} = \int_0^\infty F_{n1} ^2 dR$
1	99.98%
2	99.80%
3	99.15%
4	98.90%
5	99.21%

digits.

TABLE II: Convergence of the ground state energy as a function of the number of channels included in Eq. (7).

Number of channels	Ground state energy (mu^2/\hbar^2)
1	-2.136 033
2	-2.136 481
3	-2.136 523
4	-2.136 525
5	-2.136 526
6	-2.136 527
15	-2.136 527

In Table III we give our converged results for the ground and first four excited states (calculated with 15 channels). Is well known [20] that the hyperspherical energy obtained disregarding all couplings and the energy obtained considering only the diagonal coupling in Eq. (7) are, in fact, lower and upper bounds for the ground state energy, respectively. In these approximations, we obtained a lower bound corresponding to $-2.138\,650\,mu^2/\hbar^2$ and an upper bound of $-2.136033mu^2/\hbar^2$. The difference between them is about 0.1% while the results obtained in Ref. [12] give a differ-

ence of about 10%. By comparison, for a system like the He atom [21], where the electronic repulsion plays an important rule, the relative difference between the lower and upper bounds estimated from hyperspherical potential curves is about 1%.

TABLE III: Ground state and excited states energies $E_{n,\nu}$ ($\nu = 1$) calculated using 15 coupled channels.

n	$E_{n,\nu} \text{ (} mu^2/\hbar^2 \text{)}$
1	-2.136 527
2	-1.145 881
3	-0.786 454
4	-0.661 162
5	-0.603 740

IV. SUMMARY

We have used the adiabatic hyperspherical representation to describe system of three identical bosons with

attractive $1/r$ potentials. Such a system might eventually be created experimentally by irradiating ultracold atoms with intense, extremely off-resonant lasers. We calculated the ground state and excited state energies converged to seven digits which represents a substantial improvement over previous results. Our method is essentially exact, with the only approximation being the truncation of the number of channels used in the expansion of the total wave function. Although other methods, such as Hylleraas variational techniques, might provide much better bound states energies, as we have shown here, the adiabatic hyperspherical representation naturally offers qualitative information along with quantitative results.

Acknowledgments

This work was supported by the National Science Foundation.

-
- [1] D. O'Dell, S. Giovanazzi, G. Kurizki, and V.M. Akulin, Phys. Rev. Lett. **84**, 5687 (2000); see commentary by J. Anglin, Nature (London) **406**, 29 (2000).
 - [2] S. Giovanazzi, D. O'Dell, and G. Kurizki, Phys. Rev. A **63**, 031603(R) (2001).
 - [3] S. Giovanazzi, D. O'Dell, and G. Kurizki, Phys. Rev. Lett. **88**, 130402 (2002).
 - [4] D.-I. Choi, Phys. Rev. A **66** 063609 (2002).
 - [5] V. S. Melezhik and C.-Y. Hu, Phys. Rev. Lett. **90** 083202 (2003).
 - [6] S. Giovanazzi, G. Kurizki, I. E. Mazets, and S. Stringari, Europhys. Lett. **56**, 1 (2001).
 - [7] T. Thirunamachandran, Mol. Phys. **40**, 393 (1980); D.P. Craig and T. Thirunamachandran, *Molecular Quantum Electrodynamics* (Academic Press, London, 1984), Sec. 7.12.
 - [8] S. Inouye *et al.*, Nature (London) **392**, 151 (1998); J. Stenger *et al.*, Phys. Rev. Lett. **82**, 2422 (1999).
 - [9] X. Z. Wang, Phys. Rev. D **64** 124009 (2001).
 - [10] I.M. Moroz, R. Penrose and P. Tod, Class. Quantum Grav. **15**, 2733 (1996).
 - [11] M. E. Fisher and D. Ruelle, J. Math. Phys. **7**, 260 (1966); F. J. Dyson and A. Lenard, J. Math. Phys. **8**, 423 (1967).
 - [12] J.L. Basdevant, A. Martin and J.M. Richard, Nucl. Phys. B **343**, 60 (1990).
 - [13] B. R. Johnson, J. Chem. Phys. **73**, 5051 (1980); R. C. Whitten and F. T. Smith, J. Math. Phys. **9**, 1103 (1968);
 - [14] H. Suno, B. D. Esry, C. H. Greene and J. P. Burke, Jr., Phys. Rev. A **65**, 042725 (2002).
 - [15] H. Suno, B. D. Esry, and C. H. Greene, New J. Phys. **5**, 53 (2003).
 - [16] R.T. Pack and G.A. Parker, J. Chem. Phys. **87**, 3888 (1987).
 - [17] M.E. Rose, *Elementary Theory of Angular Momentum* (Wiley, New York, 1957), pp. 52-54.
 - [18] C. de Boor, *A Practical Guide to Splines* (Springer, New York, 1978),
 - [19] C. D. Lin, Phys. Rep. **257**, 1 (1995).
 - [20] A. F. Starace and G. L. Webster, Phys. Rev. A **19**, 1629 (1979); H. T. Coelho and J. E. Hornos, Phys. Rev. A **43**, 6379-6381 (1991).
 - [21] J. J. De Groote, M. Masili, and J. E. Hornos, J. Phys. B **31**, 4755 (1998).